The Protein Corona of PEGylated PGMA-based Nanoparticles is Preferentially Enriched with Specific Serum Proteins of Varied Biological Function

Priya S.R. Naidu[a,b], Marck Norret[a], Nicole M. Smith[a,b], Sarah A. Dunlop[b], Nicolas L. Taylor[a,c,], Melinda Fitzgerald[b,d,]*, K. Swaminathan Iyer[a,]**

[a]School of Molecular Sciences, The University of Western Australia, 35 Stirling Highway, Crawley, WA 6009, Australia

[b]School of Biological Sciences, The University of Western Australia, 35 Stirling Highway, Crawley, WA 6009, Australia

[c]ARC Centre of Excellence in Plant Energy Biology, The University of Western Australia, 35 Stirling Highway, Crawley, WA 6009, Australia

[d] Curtin Health Innovation Research Institute, Curtin University and the Perron Institute for Neurological and Translational Science, Sarich Neuroscience Research Institute, QEII Medical Centre, Nedlands WA 6009, Australia

KEYWORDS : protein corona, stealth nanoparticles, poly(glycidyl methacrylate), poly(ethylene glycol)

ABSTRACT

Composition of the protein corona formed on poly(ethylene glycol)-functionalised (PEGylated) poly(glycidyl methacrylate) (PGMA) nanoparticles (NPs) was qualitatively and quantitatively compared to the protein corona on non-PEGylated PGMA NPs. Despite the reputation of PEGylated NPs for 'stealth' functionality, we demonstrate preferential enrichment of specific serum proteins of varied biological functions in the protein corona on PEGylated NPs when compared to non-PEGylated NPs. Additionally, we suggest that the base material of polymeric NPs plays a role in the preferential enrichment of select serum proteins to the hard corona.

TEXT

Intravenously delivered, therapeutic NPs recruit circulating biomolecules found in blood plasma onto their surfaces, due to the availability of abundant surface free energy.[1] While significant advances have been made in targeted delivery of therapeutic agents using polymeric NPs, it is widely accepted that understanding the fundamental interactions of the functional NPs with serum proteins is pivotal for clinical translation. As the bulk of the physiological milieu consists of proteins, this complex biological layer formed on NPs is referred to as the protein corona.[2] The synthetic and pristine surface of NPs is transformed by components of the protein corona, endowing NPs with a biological identity[3], which can result in alterations in properties such as surface charge[4] and colloidal stability.[5] Such changes inevitably impact physiological

and pathological responses such as the incitation of pro-inflammatory effects and immunological recognition[6], moderation of biocompatibility[7] and alteration of drug release profiles.[8] Protein adsorption on NPs may also play a pivotal role in selective cellular uptake, which is fundamental to targeted therapy. The constituents of the protein corona are known to vary according to intrinsic properties such as the NP's surface chemistry[9], hydrodynamic size[10] and surface charge[4]. External conditions such as exposure temperature[11] and biological source[12] are also capable of controlling the composition of the protein corona. While some studies have reported that the protein corona does not impair targeting efficiency of therapeutic NPs[13-14], others have suggested that the adsorbed protein layer causes NPs to lose the ability to target specific cell receptors.[15-16] It has also been indicated that distinct proteins present in the corona were able to regulate cellular uptake of NPs.[17] Taken together, it is now accepted that NP biodistribution is indeed influenced by the presence of the protein corona.

NPs are often cleared rapidly from the circulation as part of immunological responses by phagocytic cells in the reticuloendothelial system (RES), due to the recruitment of plasma proteins called opsonins in the protein corona. In order to prevent RES recognition, a widely used practice in nanotherapy development is poly(ethylene glycol) (PEG) functionalisation on the NP surface.[18] PEG, with its hydrophilic polyether backbone is able to prevent non-specific protein adsorption by means of steric repulsion, thus conferring 'stealth' properties to the NPs.[19] PEGylated NPs may therefore be able to evade sequestration by the RES and increase circulation time to allow for specific cell recognition and subsequent uptake.[20] It is now understood that PEGylation does not completely eradicate protein adsorption on the NP surface; it merely serves to reduce protein interactions with increasing density of PEG grafting.[9] It is therefore pivotal to decipher the differential nature of the protein corona composition following PEGylation of

polymeric NPs. It is also important to note that this composition is variable depending on the type of polymeric NPs.[21] In this study, we have examined the influence of PEGylation using systematic analysis of the protein corona composition on PEGylated and non-PEGylated PGMA NPs. PEG chain of M_p 3000 was selected to functionalise the PGMA NPs as literature has suggested that this molecular weight falls within the range (3000-10000) that ensures that the NP's hydrodynamic radius does not dramatically increase with PEGylation while enabling the circulation half-time to be shortened.[22] Our group has previously published data to support the use of PGMA NPs in the targeted treatment of secondary degeneration that follows neurotrauma, and no evidence of toxicity was observed. However, our studies demonstrated that functionalisation of PGMA NPs was confounded, likely due to the protein corona[23-24]. As an in depth analysis of the protein corona formed on these NPs has not been conducted before, this study was designed to provide more insight to the PGMA-based NPs' therapeutic potential. In particular, we demonstrate that while it has been previously reported that the protein corona composition following PEGylation of NPs is associated with abundance of clusterin (also known as apolipoprotein J),[25] PEGylated PGMA NPs are also enriched with a range of proteins including serum albumin as well as coagulation and complement proteins from serum. We selected human serum for our experiments on the basis of potential future clinical relevance.

PGMA is a versatile polymer that can be constructed into micelles, capsules, nanoparticles and inorganic-organic hybrid materials that have immense potential in biological applications.[26] In this study, PGMA NPs conjugated with a fluorescent dye, rhodamineB (RhB) were synthesised and subsequently PEGylated (Figure 1A) according to established methods.[27] RhB was conjugated to PGMA NPs to enable their detection via fluorescence when introduced into biological environments *in vitro* and *in vivo*.[24, 28] Imaged using Transmission Electron

Microscopy (TEM), both NP preparations exhibited a mono-dispersed, spherical polymeric structure (Figure 1B), with the exception of some NPs that were overlaid on one another during the sample preparation on the TEM grids. NPs were incubated in 55% human serum at 37ºC in order to mimic *in vivo* conditions and gently washed thereafter to retain the tightly bound serum proteins on their surfaces (commonly referred to as the 'hard' corona). Quantification of the eluted hard corona proteins by bicinchoninic acid (BCA) protein assay (Figure 1C), revealed that the total protein concentration detected on PGMA-RhB NPs was ~15X greater than on PEG-PGMA-RhB. Dynamic Light Scattering (DLS) (Figure 1D) and zeta potential measurements (Figure 1E) of the NPs before and after serum incubation established that the hard corona formed and was stably retained on both NP variants. The hydrodynamic radii and polydispersity index (PDI) showed that the increase in NP size and aggregation due to protein adsorption was less in PEG-PGMA-RhB NPs than PGMA-RhB NPs. The negative change in surface charge after serum incubation for both NP variants was indicative of the mostly anionic serum proteins adsorbing onto them, likely leading to electrostatic stabilisation.[29] Collectively, it can be extrapolated that the PGMA-RhB NPs had a greater abundance of serum proteins adsorbed on their surface, causing more NP aggregation due to increased protein-protein interactions. As augmented hydrophobicity of NPs is established as an important driving force for greater protein adsorption[30], these results affirmed that PEGylation of the PGMA-based NPs to increase hydrophilicity did play a role in reducing protein adsorption on the NP surface. More importantly, it was ascertained that despite PEGylation, the PGMA-based NPs formed a stable, tightly bound protein corona on their surface upon exposure to human serum under physiological conditions, changing their physico-chemical properties.

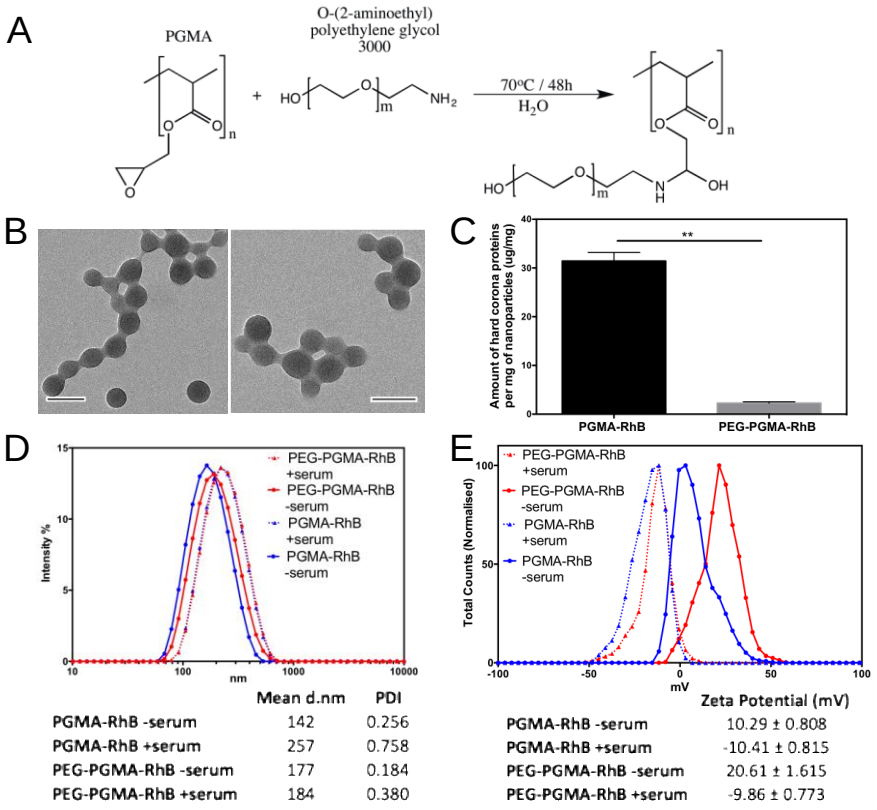

Figure 1. (A) Schematic diagram of PEGylation of PGMA-based NPs by nucleophilic epoxide ring-opening reaction. (B) TEM image of PGMA-RhB (left panel) and PEG-PGMA-RhB NPs (right panel). Scale bar = 100nm. (C) Mean ± standard error of measurement (SEM) of protein concentration of hard corona from NP variants assessed by BCA protein assay (Student's t-test, n=3, **p<0.005). (D) DLS measurements of hydrodynamic radii of NPs before and after serum incubation. Refer to Figure S3 for hydrodynamic size represented on a non-logarithmic scale. (E) Zeta potential measurements of surface charge of NP variants before and after serum incubation.

The proteins found in human serum and the hard corona samples were separated by sodium dodecyl sulphate acrylamide gel electrophoresis (SDS-PAGE) (Figure 2A) and protein band intensities were subsequently quantified using the open-source image analysis tool, ImageJ. Each lane was loaded with equal amounts of total protein so as to enable comparative quantification of individual protein abundance for each hard corona sample. A heat map (Figure 2B) generated across observed molecular weights (Bands 1-20) allowed comparison of the mean abundance of the protein bands from all samples. The general pattern indicated that the hard corona of PGMA-RhB NPs was enriched with more serum proteins than PEG-PGMA-RhB. This was observed predominantly in protein bands <54kDa. All three samples possessed a highly intense protein band at ~66kDa (Band 9) and these bands were most abundant for human serum and the PEG-PGMA-RhB sample. Along with Band 9's enriched presence, the PGMA-RhB sample also had a similarly abundant protein band at ~30kDa (Band 15). These variations in protein abundance were in accordance to the Vroman effect which describes protein adsorption on surfaces as competitive, where highly mobile and more abundant proteins in the environment, which may adsorb at earlier time points, can eventually be replaced by other proteins that possess stronger binding affinities to the material surface.[31] In this study, by allowing serum incubation to extend to 1 hour, the dynamic protein exchange processes on the NPs were allowed to reach steady-state so that proteins with the highest affinity to each NP variant were retained for analysis. We ascertained that the selected incubation period was suitable by observing the protein corona formed on these PGMA-based NPs by SDS-PAGE in a time course study (Figure S2). As indicated in literature[29], we observe that the protein corona eluted from the serum-incubated NPs did not significantly vary after the 1-hour time point and remained consistent up to 4 hours of serum incubation.

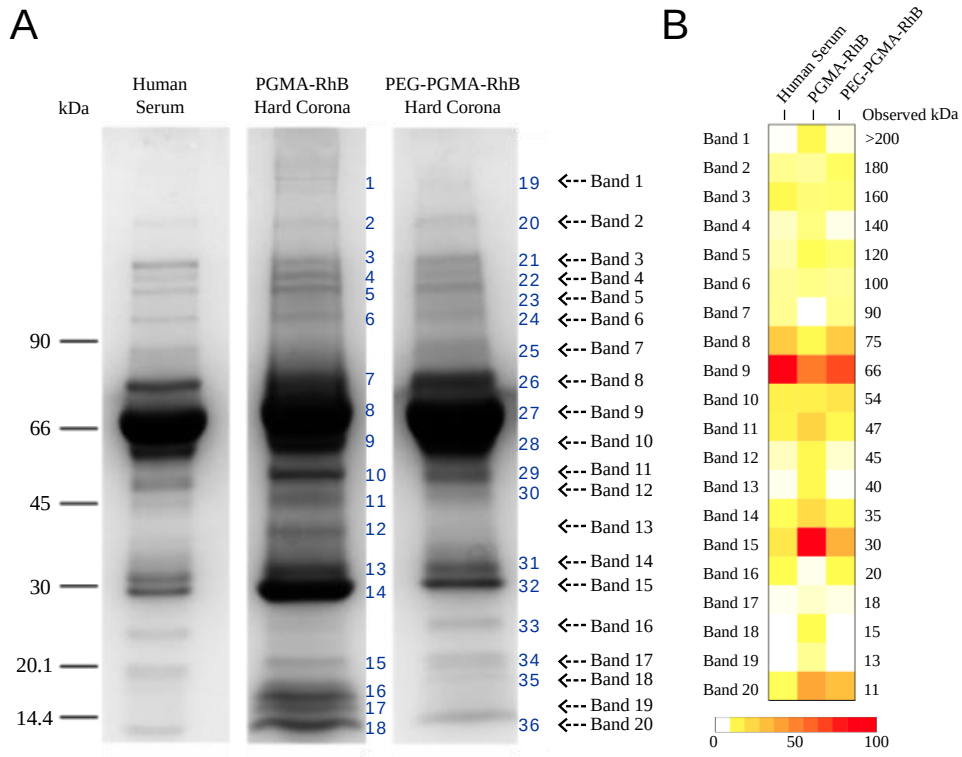

Figure 2. (A) SDS-PAGE of human serum and hard corona samples eluted from PGMA-RhB and PEG-PGMA-RhB nanoparticles. Gel spots 1-36 (in blue) were excised and subjected to in-gel digestion for liquid chromatography-mass spectrometry (LCMS) analysis. (B) Heat map of mean band abundance from analysed samples, across observed kDa in the SDS-PAGE gel. Abundance data was generated by ImageJ analysis of band intensities (Table S1) and the most intense band in human serum was normalised to the value of 100. (n=3)

Table 1. List of identified hard corona proteins on PEGylated and non-PEGylated PGMA-based NPs as detected by LCMS. MASCOT scores greater than 36 were significant ($p<0.05$). Protein IDs highlighted in blue text indicate those that were found only on respective NPs (i.e. exclusive to NP type within the sensitivity limits of the analytical tool)

NP	BAND ID	SPOT NO.	PROTEIN ID	ACCESSION NO.	THEORETICAL M_R	OBSERVED M_R	MASCOT SCORE	TOTAL SIGNIFICANT MATCHES (TOTAL UNIQUE BANDS SIGNIFICANT MATCHES)	SEQUENCE COVERAGE %
PGMA-RhB NP	1	1	APOLIPOPROTEIN B-100	P04114	515283	>200000	449	73 (29)	21
	2	2	COMPLEMENT C4B	A0A0G2JL54	187598	180000	516	32 (18)	22
			COMPLEMENT C3	P01024	187030		514	39 (26)	29
	3	3	ALPHA-1-MACROGLOBULIN	P01023	163188	160000	511	45 (27)	39
	4	4	COMPLEMENT FACTOR H	P08603	139005	140000	88	17 (6)	16
	5	5	CERULOPLASMIN	P00450	122128	120000	152	14 (8)	15
	6	6	INTER-ALPHA TRYPSIN INHIBITOR HEAVY CHAIN H1	P19827	101326	100000	116	11 (5)	18
			INTER-ALPHA TRYPSIN INHIBITOR HEAVY CHAIN H2	P19823	106590		62	11 (6)	15
	8	7	SEROTRANSFERRIN	P02787	77014	75000	345	36 (16)	38
	9	8	SERUM ALBUMIN	P02768	69321	66000	572	32 (21)	49
			C4b-BINDING PROTEIN ALPHA CHAIN	P04003	66989		136	10 (4)	19
			PROTHROMBIN	P00734	69992		97	6 (4)	10
	10	9	ANTITHROMBIN-III	P01008	52569	54000	339	18 (9)	49
			CLUSTERIN	P10909	52461		205	15 (10)	34
			PLASMA PROTEASE C1 INHIBITOR	P05155	55119		154	11 (5)	24
	11	10	ALPHA-1-ANTITRYPSIN	A0A024R6I7	46679	47000	330	26 (15)	60
			ALPHA-1-ANTICHYMOTRYPSIN	P01011	47621		107	5 (4)	16
	12	11	APOLIPOPROTEIN A-IV	P06727	45371	45000	299	32 (17)	70
	13	12	SERUM PARAOXONASE/ARYLESTERASE 1	P27169	39706	40000	363	12 (8)	52
			ACTIN, CYTOPLASMIC 1	P60709	41710		181	12 (7)	39
	14	13	APOLIPOPROTEIN E	P02649	36132	35000	232	19 (12)	65
	15	14	APOLIPOPROTEIN A-I	P02647	30759	30000	272	27 (16)	72
	17	15	TRANSTHYRETIN	P02766	15877	18000	178	9 (5)	65
	18	16	APOLIPOPROTEIN A-II	P02652	14905	15000	108	8 (5)	48
			APOLIPOPROTEIN C-IV	P55056	14543		46	3 (2)	18
	19	17	IGK KAPPA CHAIN C REGION	P01834	12988	13000	206	6 (5)	72
			APOLIPOPROTEIN C-III	P02656	12807		183	2 (1)	23
	20	18	IGK KAPPA CHAIN V-III REGION SIE	P01620	11768	11000	179	3 (3)	39
			APOLIPOPROTEIN C-III ISOFORM	P02655	11277		95	4 (3)	49
PEG-PGMA-RHB	1	19	APOLIPOPROTEIN B-100	P04114	515283	>200000	646	96 (44)	24
	2	20	COMPLEMENT C3	P01024	187030	180000	355	39 (16)	26
			COMPLEMENT C4B	A0A0G2JL54	187598		220	14 (6)	9
	3	21	ALPHA-2-MACROGLOBULIN	P01023	163188	160000	462	42 (22)	36
	4	22	COMPLEMENT FACTOR H	P08603	139005	140000	98	9 (5)	7
	5	23	CERULOPLASMIN	P00450	122128	120000	266	16 (13)	17
	6	24	INTER-ALPHA TRYPSIN INHIBITOR HEAVY CHAIN H2	P19823	105150	100000	293	20 (12)	23
			INTER-ALPHA TRYPSIN INHIBITOR HEAVY CHAIN H1	P19827	101326		224	15 (10)	21
	7	25	PLASMINOGEN	P00747	90510	90000	85	9 (4)	8
	8	26	SEROTRANSFERRIN	P02787	77014	75000	236	19 (10)	32
	9	27	SERUM ALBUMIN	P02768	69321	66000	557	33 (23)	45
	10	28	ANTITHROMBIN-III	P01008	52569	54000	317	15 (11)	39
			CLUSTERIN	P10909	52461		154	14 (7)	31
			IGG GAMMA-1 CHAIN C REGION	P01857	51880		99	13 (8)	34
	11	29	ALPHA-1-ANTITRYPSIN	A0A024R6I7	46679	47000	400	26 (15)	64
			ALPHA-1-ANTICHYMOTRYPSIN	P01011	47621		131	7 (3)	22
	12	30	APOLIPOPROTEIN A-IV	P06727	45371	45000	287	23 (13)	58
			HAPTOGLOBIN	P00738	45177		132	10 (5)	28
	13	31	SERUM PARAOXONASE/ARYLESTERASE 1	P27169	39706	40000	97	8 (6)	30
	14	32	APOLIPOPROTEIN E	P02649	36132	35000	42	2 (2)	10
	15	33	APOLIPOPROTEIN A-I	P02647	30759	30000	274	21 (13)	71
	16	34	HUMAN COMPLEMENT COMPONENT C8 GAMMA CHAIN	P07360	22264	20000	53	4 (3)	29
	17	35	TRANSTHYRETIN	P02766	15877	18000	121	7 (6)	63
	19	36	IGK KAPPA CHAIN C REGION	P01834	12988	13000	93	5 (5)	71
			APOLIPOPROTEIN C-III	P02656	12807		50	1 (1)	13
	20		IGL LAMBDA CHAIN V-III REGION LOI	P80748	11928	11000	146	4 (1)	45
			IGK KAPPA CHAIN V-III REGION SIE	P01620	11768		102	4 (2)	45

In order to provide more insight to the findings in Figure 2, gel bands, labeled 1-36, were excised for in-gel digestion to identify the hard corona proteins via LCMS. Identifications of the

hard corona proteins from both NP variants are presented in Table 1 and duly correlated to the respective Band IDs. The majority of the hard corona proteins were similar in both PGMA-RhB and PEG-PGMA-RhB NPs. This included serum albumin, which is the most abundant protein in blood plasma. However, it was noteworthy that certain proteins (highlighted in blue in Table 1) appeared to be exclusive to the hard corona of each NP variant, within the limit of sensitivity of the detection methods employed. The selective presence of specific serum proteins on each NP type suggested that physico-chemical differences between NPs could have enabled the exclusive recruitment of serum proteins onto their surfaces.

Table 2. One-way ANOVA analysis indicating the significance of the differences of individual protein band abundance of human serum and hard corona samples. (n = 3, *p<0.05, **p<0.005, ***p<0.0005, ****p<0.00005, HS = human serum, ns = no significance, NA = no preferential adsorption of protein was determined from this analysis, # = apparent preferential adsorption to specific NP and @ = apparent exclusive presence of protein to specific NP, within the limits of sensitivity of the assay.) Graphical representation of the statistical analysis can be found in Figure S4.

Band ID	HS vs. PGMA-RhB	HS vs. PEG-PGMA-RhB	PGMA-RhB vs. PEG-PGMA-RhB	Protein ID	Apparent Preferential[#] or Exclusive[@] Adsorption
1	****	ns	****	Apolipoprotein B-100	PGMA-RhB[#]
2	ns	**	**	Complement C3	PEG-PGMA-RhB[#]
				Complement C4b	PEG-PGMA-RhB[#]
3	****	***	ns	Alpha-1-macroglobulin	PEG-PGMA-RhB[#]
4	***	*	***	Complement Factor H	PGMA-RhB[#]
5	***	**	*	Ceruloplasmin	PGMA-RhB[#]
6	ns	ns	ns	Inter-alpha trypsin inhibitor heavy chain H1	NA
				Inter-alpha trypsin inhibitor heavy chain H2	NA
7	****	ns	****	Plasminogen	PEG-PGMA-RhB[@]
8	****	ns	****	Serotransferrin	PEG-PGMA-RhB[#]
9	****	***	**	Serum Albumin	PEG-PGMA-RhB[#]
				C4b-binding protein alpha chain	PGMA-RhB[@]
				Prothrombin	PGMA-RhB[@]
10	ns	**	*	Antithrombin-III	PEG-PGMA-RhB[#]
				Clusterin	PEG-PGMA-RhB[#]
				Ig gamma-1 chain C region	PEG-PGMA-RhB[@]
				Plasma protease C1 inhibitor	PGMA-RhB[@]
11	***	ns	***	Alpha-1-antitrypsin	PGMA-RhB[#]
				Alpha-1-antichymotrypsin	PGMA-RhB[#]
12	****	ns	****	Apolipoprotein A-IV	PGMA-RhB[#]
				Haptoglobin	PEG-PGMA-RhB[@]
13	****	ns	****	Serum paraoxonase/arylesterase 1	PGMA-RhB[#]
				Actin, Cytoplasmic 1	PGMA-RhB[@]
14	***	ns	***	Apolipoprotein E	PGMA-RhB[#]
15	****	***	****	Apolipoprotein A-I	PGMA-RhB[#]
16	****	*	****	Human complement component C8 gamma chain	PEG-PGMA-RhB[@]
17	****	*	***	Transthyretin	PGMA-RhB[#]
18	****	ns	****	Apolipoprotein A-II	PGMA-RhB[@]
				Apolipoprotein C-IV	PGMA-RhB[@]
19	****	ns	****	Ig kappa chain C region	PGMA-RhB[#]
				Apolipoprotein C-III	PGMA-RhB[#]
20	****	****	*	Ig kappa chain V-III region SIE	PGMA-RhB[@]
				Apolipoprotein C-III isoform	PGMA-RhB[@]
				Ig lambda chain V-III region LOI	PEG-PGMA-RhB[@]

Statistical analysis of the band intensities compared the abundance of proteins in human serum and the hard corona samples. 1-way ANOVA was performed on normalised protein band

intensity data (Tables S1, S2 and Figure S4) to determine if individual proteins found in human serum adsorbed preferentially, rather than exclusively, on either PEGylated or non-PEGylated PGMA-based NPs i.e. whether there were significant differences in the abundance of hard corona proteins common to both NP variants. The dynamic exchanges between various serum proteins and NP surfaces involved in the formation of a stable hard corona are currently poorly understood. This analysis, which combined proteomics data and statistical processing, was conducted to elucidate if select proteins could be preferentially retained within the hard corona of nanoparticles with different surface functionalisation upon the stabilisation of protein interactions. The results from this analysis are summarised in Table 2. From Table 1, it was observed that bands 6, 9-11, 13 and 18-20 were a combination of serum proteins of similar molecular weights, which precluded single protein identification and the generation of individual protein abundance values. Nevertheless, combining the data from Table 1 and Figure S4 provided the necessary evidence to establish that NPs used in this study, PEGylated or otherwise, harnessed certain serum proteins preferentially to the hard corona. Amongst the proteins that were detected in both hard corona samples, the more hydrophobic PGMA-RhB NPs indicated apparent preferential adsorption of twelve proteins including apolipoprotein B-100, complement factor H, ceruloplasmin, alpha-1-antitrypsin, alpha-1-antichymotrypsin, apolipoprotein A-IV, serum paraoxonase/arylesterase I, apolipoprotein E, apolipoprotein A-I, transthyretin, Ig kappa chain C region and apolipoprotein C-III. It was interesting to observe the apparent preferential adsorption of seven proteins such as complements C3 and C4b, alpha-1-macroglobulin, serotransferrin, serum albumin, antithrombin-III as well as clusterin on the PEGylated NPs. This finding showed that despite PEGylation being a typical and widely used practice to reduce protein interactions on NP surfaces, select serum proteins could still accumulate on them with

proclivity. It has been suggested that the dynamic process of protein corona formation could leave 'fingerprints' of initially adsorbed proteins on the NP surface which could go on to influence subsequent protein adsorption.[21, 32-33] The current demonstration of apparent preferential adsorption of serum proteins resonates with this idea, suggesting that a variation in surface functionalisation of the NP, such as PEGylation, could invoke a cascade of protein interactions specific to the NP surface properties that would influence hard corona composition.

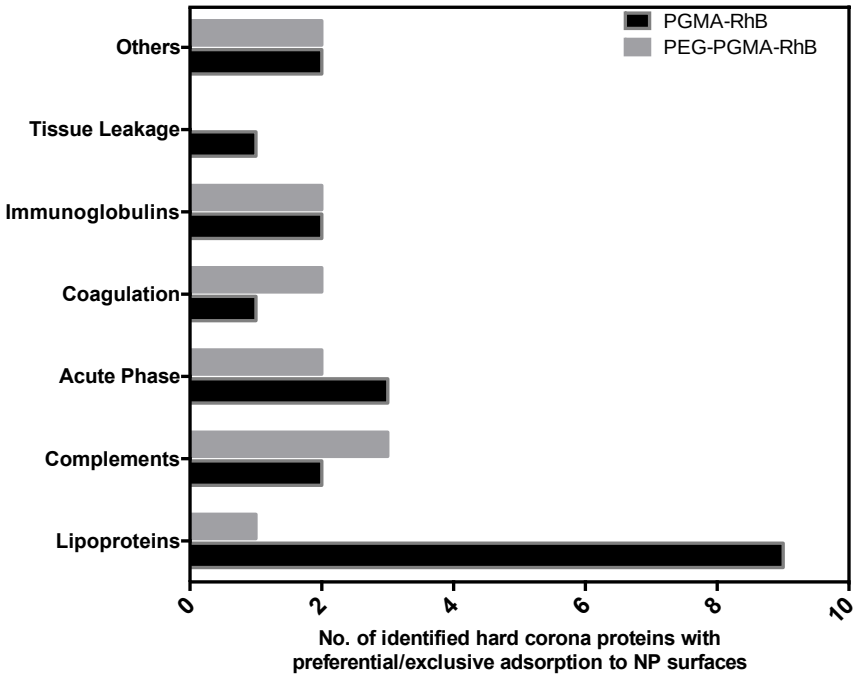

Figure 3. Classification of hard corona proteins from PEGylated and non-PEGylated PGMA-based NPs according to their biological functions, as ascertained by the PANTHER classification system.

Since the presence of the protein corona may enable protein-specific NP behaviour, the hard corona proteins that were either preferentially or exclusively adsorbed on each NP variant were classified according to their biological functions (Figure 3), using the open-source PANTHER classification system.[34] Notably, it was revealed that PGMA-RhB NP surfaces were enriched

appreciably by lipoproteins. Lipoproteins are extensively involved in lipid and cholesterol binding, transport and metabolism. Some of them have been reported to promote targeting *in vivo*. For example, apolipoprotein E has promoted NP transport across the blood-brain barrier[35], while both apolipoprotein A-I and apolipoprotein B-100 have improved the transport of NPs into the central nervous system.[36] This may suggest that the lipoprotein-rich hard corona surrounding PGMA-RhB NPs could potentially direct improved corona-mediated targeting and/or central nervous system biodistribution *in vivo*. Opsonins such as immunoglobulins, acute phase and complement proteins were present on both hard corona samples. While immunoglobulins impartially amassed on both NP variants, the PEGylated NPs were distinguished by amplified enrichment of complement and coagulation proteins in comparison to the non-PEGylated NPs. These findings may assist in explaining the instances of PEG-specific immune responses and blood clotting associated with PEG presence in the physiological system.[37] In summary, preferential accumulation of proteins of significant biological functions on NP variants used in this study suggested that the resulting hard corona could still permit them to engage in specific cellular activity despite 'stealth-like' functionalisations, thereby potentially governing NP behaviour *in vivo*.

Studies have previously described the use of 'stealth'-motivated PEGylated nanocarriers in targeted therapy and it had not gone unnoticed that the protein corona could control their fate *in vivo*.[38] A recent report using polystyrene NPs revealed that the stealth effect was in fact promoted by the augmented abundance of clusterin in the hard corona.[25] Here, it was observed that while clusterin did preferentially adsorb on PEGylated PGMA-based NPs, it was present along with other serum proteins as previously noted. It is therefore suggested that variations in

the base material used in the NP formulation could regulate the protein corona profile and thereby impact the NPs' subsequent interactions with the physiological environment.

ASSOCIATED CONTENT

Supporting Information. FTIR spectrum confirming PEGylation of nanoparticles, time-based gel electrophoresis of protein corona from nanoparticle variants, hydrodynamic radii measurements by dynamic light scattering in non-logarithmic scale, raw data of protein band abundance, statistical processing data of protein band abundance and graphical representation of band abundance from protein corona and human serum samples are available in the supporting information document.

AUTHOR INFORMATION

Corresponding Author

* nicolas.taylor@uwa.edu.au, lindy.fitzgerald@curtin.edu.au, swaminatha.iyer@uwa.edu.au

Author Contributions

The manuscript was written through contributions of all authors. All authors have given approval to the final version of the manuscript.

ACKNOWLEDGMENT

This work was funded by the Australian Research Council (ARC) and the National Health & Medical Research Council (NHMRC) of Australia (APP1082403 and APP1087114). Dr. Nicolas L. Taylor is funded as an ARC Future Fellow (FT13010123). The authors would also like to

acknowledge the assistance received from Miss Nicole Hortin and Ms. Wissam Chiha (Experimental and Regenerative Neurosciences (EaRN) division of the School of Animal Biology) from the University of Western Australia for assistance with development of techniques and helpful discussions.

ABBREVIATIONS

ACN, Acetonitrile; AIBN, azobisisobutyronitrile; Ar, Argon; BCA, Bicinchoninic acid; DLS, Dynamic Light Scattering; HS, Human Serum; GMA, Glycidyl methacrylate; FA, Formic acid; FTIR, Fourier Transform Infra-Red; LCMS, Liquid Chromatography Mass Spectrometry; MEK, Methyl ethyl ketone; NP, Nanoparticle; PBS, Phosphate Buffered Saline; PEG, Polyethylene glycol; PGMA, Poly(glycidyl methacrylate); RhB, RhodamineB; RT, Room temperature; SDS-PAGE, Sodium dodecyl sulphate polyacrylamide gel electrophoresis; TEM, Transmission Electron Microscopy; TFA, trifluoroacetic acid; THF, Tetrahydrofuran; Tris, Tris(hydroxymethyl)aminomethane

REFERENCES

1. Tenzer, S.; Docter, D.; Kuharev, J.; Musyanovych, A.; Fetz, V.; Hecht, R.; Schlenk, F.; Fischer, D.; Kiouptsi, K.; Reinhardt, C.; Landfester, K.; Schild, H.; Maskos, M.; Knauer, S. K.; Stauber, R. H., Rapid formation of plasma protein corona critically affects nanoparticle pathophysiology. *Nat Nano* **2013,** *8* (10), 772-781.

2. Lynch, I.; Cedervall, T.; Lundqvist, M.; Cabaleiro-Lago, C.; Linse, S.; Dawson, K. A., The nanoparticle–protein complex as a biological entity; a complex fluids and surface science challenge for the 21st century. *Advances in Colloid and Interface Science* **2007,** *134–135*, 167-174.

3. Docter, D.; Strieth, S.; Westmeier, D.; Hayden, O.; Gao, M.; Knauer, S. K.; Stauber, R. H., No king without a crown – impact of the nanomaterial-protein corona on nanobiomedicine. *Nanomedicine* **2015,** *10* (3), 503-519.

4. Calatayud, M. P.; Sanz, B.; Raffa, V.; Riggio, C.; Ibarra, M. R.; Goya, G. F., The effect of surface charge of functionalized Fe_3O_4 nanoparticles on protein adsorption and cell uptake. *Biomaterials* **2014,** *35* (24), 6389-6399.

5. Gebauer, J. S.; Malissek, M.; Simon, S.; Knauer, S. K.; Maskos, M.; Stauber, R. H.; Peukert, W.; Treuel, L., Impact of the nanoparticle–protein corona on colloidal stability and protein structure. *Langmuir* **2012,** *28* (25), 9673-9679.

6. Deng, Z. J.; Liang, M.; Monteiro, M.; Toth, I.; Minchin, R. F., Nanoparticle-induced unfolding of fibrinogen promotes Mac-1 receptor activation and inflammation. *Nat Nano* **2011,** *6* (1), 39-44.

7. Landgraf, L.; Christner, C.; Storck, W.; Schick, I.; Krumbein, I.; Dähring, H.; Haedicke, K.; Heinz-Herrmann, K.; Teichgräber, U.; Reichenbach, J. R.; Tremel, W.; Tenzer, S.; Hilger, I., A plasma protein corona enhances the biocompatibility of $Au@Fe_3O_4$ Janus particles. *Biomaterials* **2015,** *68*, 77-88.

8. Behzadi, S.; Serpooshan, V.; Sakhtianchi, R.; Müller, B.; Landfester, K.; Crespy, D.; Mahmoudi, M., Protein corona change the drug release profile of nanocarriers: The “overlooked” factor at the nanobio interface. *Colloids and Surfaces B: Biointerfaces* **2014,** *123*, 143-149.

9. Walkey, C. D.; Olsen, J. B.; Guo, H.; Emili, A.; Chan, W. C. W., Nanoparticle size and surface chemistry determine serum protein adsorption and macrophage uptake. *Journal of the American Chemical Society* **2012,** *134* (4), 2139-2147.

10. Hu, Z.; Zhang, H.; Zhang, Y.; Wu, R. a.; Zou, H., Nanoparticle size matters in the formation of plasma protein coronas on Fe_3O_4 nanoparticles. *Colloids and Surfaces B: Biointerfaces* **2014,** *121*, 354-361.

11. Mahmoudi, M.; Abdelmonem, A. M.; Behzadi, S.; Clement, J. H.; Dutz, S.; Ejtehadi, M. R.; Hartmann, R.; Kantner, K.; Linne, U.; Maffre, P.; Metzler, S.; Moghadam, M. K.; Pfeiffer, C.; Rezaei, M.; Ruiz-Lozano, P.; Serpooshan, V.; Shokrgozar, M. A.; Nienhaus, G. U.; Parak, W. J., Temperature: The "ignored" factor at the nanobio interface. *ACS Nano* **2013,** *7* (8), 6555-6562.

12. Schottler, S.; Klein, K.; Landfester, K.; Mailander, V., Protein source and choice of anticoagulant decisively affect nanoparticle protein corona and cellular uptake. *Nanoscale* **2016**.

13. Dai, Q.; Yan, Y.; Ang, C.-S.; Kempe, K.; Kamphuis, M. M. J.; Dodds, S. J.; Caruso, F., Monoclonal antibody-functionalized multilayered particles: Targeting cancer cells in the presence of protein coronas. *ACS Nano* **2015,** *9* (3), 2876-2885.

14. Kang, B.; Okwieka, P.; Schöttler, S.; Winzen, S.; Langhanki, J.; Mohr, K.; Opatz, T.; Mailänder, V.; Landfester, K.; Wurm, F. R., Carbohydrate-based nanocarriers exhibiting specific cell targeting with minimum influence from the protein corona. *Angewandte Chemie International Edition* **2015,** *54* (25), 7436-7440.

15. Salvati, A.; Pitek, A. S.; Monopoli, M. P.; Prapainop, K.; Bombelli, F. B.; Hristov, D. R.; Kelly, P. M.; Aberg, C.; Mahon, E.; Dawson, K. A., Transferrin-functionalized nanoparticles lose their targeting capabilities when a biomolecule corona adsorbs on the surface. *Nat Nano* **2013,** *8* (2), 137-143.

16. Varnamkhasti, B. S.; Hosseinzadeh, H.; Azhdarzadeh, M.; Vafaei, S. Y.; Esfandyari-Manesh, M.; Mirzaie, Z. H.; Amini, M.; Ostad, S. N.; Atyabi, F.; Dinarvand, R., Protein corona hampers targeting potential of MUC1 aptamer functionalized SN-38 core–shell nanoparticles. *International Journal of Pharmaceutics* **2015,** *494* (1), 430-444.

17. Ritz, S.; Schöttler, S.; Kotman, N.; Baier, G.; Musyanovych, A.; Kuharev, J.; Landfester, K.; Schild, H.; Jahn, O.; Tenzer, S.; Mailänder, V., Protein corona of nanoparticles: Distinct proteins regulate the cellular uptake. *Biomacromolecules* **2015,** *16* (4), 1311-1321.

18. Pozzi, D.; Colapicchioni, V.; Caracciolo, G.; Piovesana, S.; Capriotti, A. L.; Palchetti, S.; De Grossi, S.; Riccioli, A.; Amenitsch, H.; Lagana, A., Effect of polyethyleneglycol (PEG) chain length on the bio-nano-interactions between PEGylated lipid nanoparticles and biological fluids: from nanostructure to uptake in cancer cells. *Nanoscale* **2014,** *6* (5), 2782-2792.

19. Wang, T.; Chen, Q.; Lu, H.; Li, W.; Li, Z.; Ma, J.; Gao, H., Shedding PEG palisade by temporal photostimulation and intracellular reducing milieu for facilitated intracellular trafficking and DNA release. *Bioconjugate Chemistry* **2016,** *27* (8), 1949-1957.

20. Pearson, R. M.; Juettner, V. V.; Hong, S., Biomolecular corona on nanoparticles: a survey of recent literature and its implications in targeted drug delivery. *Frontiers in Chemistry* **2014,** *2*, 108.

21. Monopoli, M. P.; Aberg, C.; Salvati, A.; Dawson, K. A., Biomolecular coronas provide the biological identity of nanosized materials. *Nat Nano* **2012,** *7* (12), 779-786.

22. Jokerst, J. V.; Lobovkina, T.; Zare, R. N.; Gambhir, S. S., Nanoparticle PEGylation for imaging and therapy. *Nanomedicine (London, England)* **2011,** *6* (4), 715-728.

23. Evans, C. W.; Viola, H. M.; Ho, D.; Hool, L. C.; Dunlop, S. A.; Fitzgerald, M.; Iyer, K. S., Nanoparticle-mediated internalisation and release of a calcium channel blocker. *RSC Advances* **2012,** *2* (23), 8587-8590.

24. Lozić, I.; Hartz, R. V.; Bartlett, C. A.; Shaw, J. A.; Archer, M.; Naidu, P. S. R.; Smith, N. M.; Dunlop, S. A.; Iyer, K. S.; Kilburn, M. R.; Fitzgerald, M., Enabling dual cellular destinations of polymeric nanoparticles for treatment following partial injury to the central nervous system. *Biomaterials* **2016,** *74*, 200-216.

25. Schöttler, S.; Becker, G.; Winzen, S.; Steinbach, T.; Mohr, K.; Landfester, K.; Mailänder, V.; Wurm, F. R., Protein adsorption is required for stealth effect of poly(ethylene glycol)- and poly(phosphoester)-coated nanocarriers. *Nat Nano* **2016,** *11* (4), 372-377.

26. Li, Q.-L.; Gu, W.-X.; Gao, H.; Yang, Y.-W., Self-assembly and applications of poly(glycidyl methacrylate)s and their derivatives. *Chemical Communications* **2014,** *50* (87), 13201-13215.

27. Tsyalkovsky, V.; Klep, V.; Ramaratnam, K.; Lupitskyy, R.; Minko, S.; Luzinov, I., Fluorescent reactive core–shell composite nanoparticles with a high surface concentration of epoxy functionalities. *Chemistry of Materials* **2008,** *20* (1), 317-325.

28. Evans, C. W.; Fitzgerald, M.; Clemons, T. D.; House, M. J.; Padman, B. S.; Shaw, J. A.; Saunders, M.; Harvey, A. R.; Zdyrko, B.; Luzinov, I.; Silva, G. A.; Dunlop, S. A.; Iyer, K. S., Multimodal analysis of PEI-mediated endocytosis of nanoparticles in neural cells. *ACS Nano* **2011,** *5* (11), 8640-8648.

29. Barrán-Berdón, A. L.; Pozzi, D.; Caracciolo, G.; Capriotti, A. L.; Caruso, G.; Cavaliere, C.; Riccioli, A.; Palchetti, S.; Laganà, A., Time evolution of nanoparticle–protein corona in human plasma: Relevance for targeted drug delivery. *Langmuir* **2013,** *29* (21), 6485-6494.

30. Walkey, C. D.; Chan, W. C. W., Understanding and controlling the interaction of nanomaterials with proteins in a physiological environment. *Chemical Society Reviews* **2012,** *41* (7), 2780-2799.

31. Vroman, L., Effect of adsorbed proteins on the wettability of hydrophilic and hydrophobic solids. *Nature* **1962,** *196* (4853), 476-477.

32. Walkey, C. D.; Olsen, J. B.; Song, F.; Liu, R.; Guo, H.; Olsen, D. W. H.; Cohen, Y.; Emili, A.; Chan, W. C. W., Protein corona fingerprinting predicts the cellular interaction of gold and silver nanoparticles. *ACS Nano* **2014,** *8* (3), 2439-2455.

33. Lundqvist, M.; Stigler, J.; Cedervall, T.; Berggård, T.; Flanagan, M. B.; Lynch, I.; Elia, G.; Dawson, K., The evolution of the protein corona around nanoparticles: A test study. *ACS Nano* **2011,** *5* (9), 7503-7509.

34. Mi, H.; Poudel, S.; Muruganujan, A.; Casagrande, J. T.; Thomas, P. D., PANTHER version 10: expanded protein families and functions, and analysis tools. *Nucleic Acids Research* **2016,** *44* (D1), D336-D342.

35. Zensi, A.; Begley, D.; Pontikis, C.; Legros, C.; Mihoreanu, L.; Wagner, S.; Büchel, C.; von Briesen, H.; Kreuter, J., Albumin nanoparticles targeted with Apo E enter the CNS by transcytosis and are delivered to neurones. *Journal of Controlled Release* **2009,** *137* (1), 78-86.

36. Kreuter, J.; Hekmatara, T.; Dreis, S.; Vogel, T.; Gelperina, S.; Langer, K., Covalent attachment of apolipoprotein A-I and apolipoprotein B-100 to albumin nanoparticles enables drug transport into the brain. *Journal of Controlled Release* **2007,** *118* (1), 54-58.

37. Knop, K.; Hoogenboom, R.; Fischer, D.; Schubert, U. S., Poly(ethylene glycol) in drug delivery: Pros and cons as well as potential alternatives. *Angewandte Chemie International Edition* **2010,** *49* (36), 6288-6308.

38. Dai, Q.; Walkey, C.; Chan, W. C. W., Polyethylene glycol backfilling mitigates the negative impact of the protein corona on nanoparticle cell targeting. *Angewandte Chemie International Edition* **2014,** *53* (20), 5093-5096.